

## NUMERICAL MODELLING OF AUSTENITE-FERRITE TRANSFORMATION IN ADI

OLEJARCZYK-WOŹEŃSKA Izabela, ADRIAN Henryk, MRZYGLÓD Barbara,  
GŁOWACKI Mirosław

*AGH University of Science and Technology, Faculty of Metals Engineering and Industrial Computer Science,  
Cracow, Poland, EU, [iolejarc@agh.edu.pl](mailto:iolejarc@agh.edu.pl)*

### Abstract

The heat treatment process of ductile iron involves two stages: austenitising at temperatures in the range of 850-950°C with the following austempering of alloy in the temperature range of 250-380°C. The resulting microstructure contains ferrite saturated with carbon in a matrix of reacted high-carbon austenite with spheroidal graphite typical of ductile iron. This microstructure confers high mechanical properties to the alloy. The microstructure and mechanical properties of ADI depend on the kinetics of phase transformations during austempering.

The kinetic model of phase transformations occurring during austempering of undercooled austenite in ADI was developed. The model is based on Fick's diffusion laws. The differential equations were solved by the Finite Difference Method (explicit scheme) under the boundary conditions adequate for the austempering temperature. In calculations, the effect of carbon content in austenite on its diffusion coefficient was considered. The developed model and computer program enabled tracing the process of ausferrite growth. Using the developed computer program, the effect of isothermal annealing temperature on the growth rate of ferritic phase was investigated.

**Keywords:** Austempering, ADI, modelling of phase transformations

### 1. INTRODUCTION

ADI (Austempered Ductile Iron) is a variation of ductile iron with a ferritic-austenitic matrix structure, characterized by a favourable combination of high strength, satisfactory ductility and fracture toughness. A wide range of the ADI mechanical properties is achieved by properly selected cycle of heat treatment leading to the formation of final microstructure, which is a mixture of stable austenite and lamellar ferrite in the form of "needles" (ausferrite). The type of the microstructure obtained is to a great extent controlled by the chemical composition of the base ductile iron and parameters of the heat treatment process. This process consists of austenitizing in the temperature range of 800 - 950 °C (pearlite - austenite transformation) and austempering in the temperature range of 230-400 °C (austenite - ferrite transformation) [1-5].

Computer modelling methods are an important tool aiding the optimization process of the Fe-C alloys microstructure and properties [6-8]. Computer simulations allow reproducing with the use of mathematical models the course of industrial processes and analysis of properties of the tested materials conducted in a manner identical with the actual process. Computer technologies, being currently available as a cheap and effective way of optimization, are used for modelling and analysis of phenomena occurring in many areas of research [6 - 16]. The numerical models developed by the authors in the first stage of the heat treatment of ductile iron to obtain ADI were described, among others, in [7, 8].

This paper presents a model of the austenite - ferrite transformation considered as a means to support the analysis of an impact of the austempering process parameters (time and temperature) on the growth rate of ferritic bainite produced as a result of the transformation.

## 2. MODEL OF AUSTENITE - FERRITE TRANSFORMATION

### 2.1. Mathematical model

The numerical model describing the kinetics of the transformation of austenite into ferrite during austempering uses the diffusion equation (Fick's second law). The model analyzes the diffusion of carbon atoms between the plates of austenite and ferrite. The analysis is based on a quantitative approach to the problem of carbon atoms diffusion in an austenite - ferrite system resulting from changes under thermodynamic conditions - from the temperature of austenitizing to the temperature of isothermal annealing. The resulting concentration gradients are responsible for the movement of phase boundaries and growth of ferrite at the expense of austenite and also for an increase in the saturation ratio of austenite with carbon [17].

Model investigations were carried out on a half ausferrite plate (**Fig. 1**).

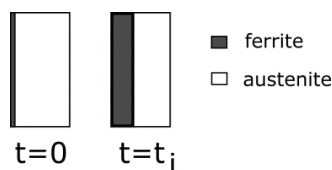


**Fig. 1** Diagram of the ausferritization process

The model ignores the rate of ferrite nucleation and diffusion of carbon atoms in between the graphite and the matrix. The process of transformation is controlled by the diffusion of carbon in austenite and ferrite. **Fig. 2** shows a scheme of the distribution of carbon concentration during the growth of ferrite in austenite [17].

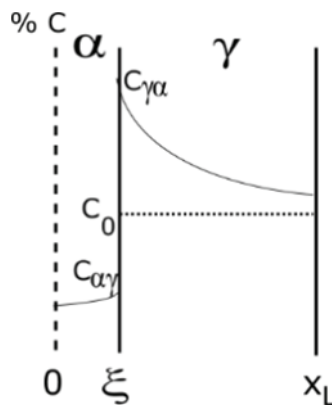


**Fig. 2** Scheme of the distribution of carbon concentration in ferrite and austenite

In this model, the growth of ferrite has been described with a system of equations (1) - (3).

$$\frac{\partial C}{\partial \tau} = D_C^\gamma \frac{\partial^2 C_\gamma}{\partial x^2} \quad (1)$$

$$\frac{\partial C}{\partial \tau} = D_C^\alpha \frac{\partial^2 C_\alpha}{\partial x^2} \quad (2)$$

$$(C_{\alpha/\gamma}\rho_\alpha - C_{\gamma/\alpha}\rho_\gamma) V_{\alpha\gamma} = D_C^\gamma \rho_\gamma \left( \frac{\partial C}{\partial x} \right)_{x=\xi^+} - D_C^\alpha \rho_\alpha \left( \frac{\partial C}{\partial x} \right)_{x=\xi^-} \quad (3)$$

where:  $C_\gamma, C_\alpha$  - is the content of carbon in austenite and ferrite, respectively,  $D_C^\gamma, D_C^\alpha$  - is the coefficient of carbon diffusion in austenite and ferrite, respectively,  $V_{\alpha\gamma}$  - is the rate of movement of the ferrite - austenite ( $\alpha/\gamma$ ) interface,  $\rho_\gamma$  - is the density of austenite (8,22 g/cm<sup>3</sup>),  $\rho_\alpha$  - is the density of ferrite (7,86 g/cm<sup>3</sup>).

The change of the carbon content in austenite and ferrite as a function of time and distance is illustrated by equations (1) and (2), respectively, while equation (3) describes the mass balance at the austenite / ferrite ( $\gamma/\alpha$ ) interface and allows determination of the rate of interface migration.

The initial conditions include the initial thickness of the plates of austenite  $l_\gamma$  and ferrite  $l_\alpha$ , and carbon content distribution in individual phases. Boundary conditions are described by equations (4) - (6).

$$C = C_{\alpha/\gamma}, \quad x = \xi^+; \quad C = C_{\gamma/\alpha}, \quad x = \xi^- \quad (4)$$

$$\frac{\partial C_\alpha}{\partial x} = 0, \quad x = 0 \quad (5)$$

$$\frac{\partial C_\gamma}{\partial x} = 0, \quad x = l_\gamma \quad (6)$$

## 2.2. Numerical solutions

Onto the area of ferrite and austenite were imposed the respective uniform meshes with  $M$  and  $M1$  nodes by dividing the area of both phases into  $M - 1$  and  $M1 - 1$  sections of the original length of  $\Delta x_\alpha = l_\alpha / (M - 1)$  and  $\Delta x_\gamma = l_\gamma / (M1 - 1)$ , respectively, (Fig. 3)

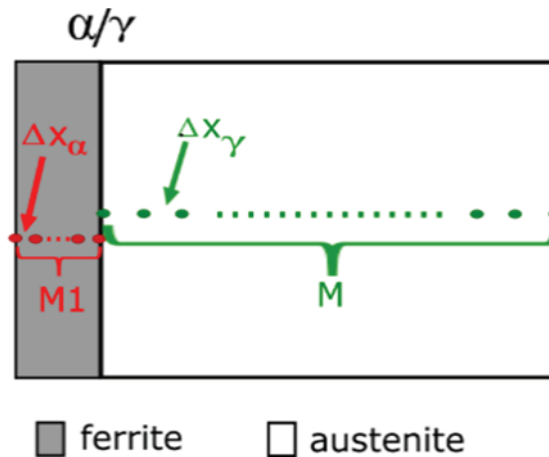


Fig. 3 Diagram of the mesh of nodes in the austenite and ferrite

Equations (1) and (2) describing changes of the carbon content in austenite and ferrite were solved by the finite difference method. In the course of calculations, the number of nodes remained constant, while the distance between them was changing. To account for the movement of nodes as a function of time, a variable Murray - Landis grid was applied [19]. For this purpose, to the equations expressing the change of carbon content, the rate of movement of the  $m$ -th node was introduced ( $V_m$ ). The differential form (explicit scheme) of changes of the carbon content in austenite and ferrite is represented by equations (7) and (8), respectively:

$$\frac{\partial C_{\gamma i}^{k+1} - C_{\gamma i}^k}{\Delta \tau} = D_c^\gamma \frac{C_{\gamma i+1}^k - 2C_{\gamma i}^k + C_{\gamma i-1}^k}{\Delta x_\gamma^2} + V_{\gamma m} \left( \frac{C_{\gamma i+1}^k - C_{\gamma i-1}^k}{2\Delta x_\gamma} \right) \quad (7)$$

$$\frac{\partial C_{\alpha j}^{k+1} - C_{\alpha j}^k}{\Delta \tau} = D_c^\alpha \frac{C_{\alpha j+1}^k - 2C_{\alpha j}^k + C_{\alpha j-1}^k}{\Delta x_\alpha^2} + V_{\alpha m} \left( \frac{C_{\alpha j+1}^k - C_{\alpha j-1}^k}{2\Delta x_\alpha} \right) \quad (8)$$

The rate of movement of the grid nodes in austenite ( $V_{\gamma m}$ ) is represented by equation (9), and in ferrite ( $V_{\alpha m}$ ) by equation (10):

$$V_{\gamma m} = \frac{x_L - x_{\gamma i}}{x_L - \xi} V_{\alpha \gamma} \quad (9)$$

$$V_{\alpha m} = \frac{x_{\alpha j}}{\xi} V_{\alpha \gamma} \quad (10)$$

where:  $x_L$  - is the actual thickness of the austenite plate,  $x_{\gamma i}$ ,  $x_{\alpha j}$  - is the position of actual points in austenite and ferrite, respectively.

The carbon mass balance equation at the austenite / ferrite interface (equation (3)) is solved with the symmetric difference quotient of carbon concentration derivative at the interface (equation (11)):

$$V_{\alpha m}(C_{\alpha \gamma} \rho_{\alpha} - C_{\gamma \alpha} \rho_{\gamma}) = D_C^{\gamma} \rho_{\gamma} \left( \frac{-3C_{\gamma[1]} + 4C_{\gamma[2]} - C_{\gamma[3]}}{2\Delta x_{\gamma}} \right) - D_C^{\alpha} \rho_{\alpha} \left( \frac{3C_{\alpha[M]} - 4C_{\alpha[M-1]} + C_{\alpha[M-2]}}{2\Delta x_{\alpha}} \right) \quad (11)$$

### 2.3. Physical data

Preliminary calculations were carried out for the initial thickness of an austenite plate equal to 10  $\mu\text{m}$  and for the ferrite plate equal to 10<sup>-4</sup>  $\mu\text{m}$ . Technical literature [17] for the calculation of diffusion coefficient typically uses its temperature-related dependence (equations (12) and (13)). The developed program also uses the temperature dependence of  $D_C^{\alpha}$  and  $D_C^{\gamma}$ . In austenite, the carbon diffusion coefficient was also calculated taking into account not only the effect of temperature but also the effect of carbon content,  $D(C, T)$  [8, 19].

$$D_C^{\gamma} = 1.67 \cdot 10^{-2} \exp\left(\frac{-1.20 \cdot 10^5}{RT}\right) \quad (12)$$

$$D_C^{\alpha} = 7.90 \cdot 10^{-3} \exp\left(\frac{-7.58 \cdot 10^4}{RT}\right) \quad (13)$$

where:  $R$  - is the gas constant,  $J/(mol \cdot K)$ ,  $T$  - is the temperature,  $K$ ,  $D_C^{\gamma}$ ,  $D_C^{\alpha}$  - are the diffusion coefficients in austenite and ferrite, respectively,  $\text{cm}^2/\text{s}$ .

Carbon content in the austenite/ferrite and ferrite/austenite interface is determined from the Fe-C phase equilibrium diagrams by digitizing the GS (Ac3) and GP lines and - assuming linearity of lines the carbon content- temperature relationship is presented by equations (15) and (16):

$$C_{\alpha/\gamma} = 0.1135 - 1.22 \cdot 10^{-4} T \quad (15)$$

$$C_{\gamma/\alpha} = 3.4463 - 3.779 \cdot 10^{-3} T \quad (16)$$

where:  $T$  - is the temperature,  $^{\circ}\text{C}$

## 3. RESULTS OF SIMULATION OF FERRITE GRAIN GROWTH DURING AUSTEMPERING

The discussed mathematical model of pearlite transformation into austenite has been implemented in Pascal language in the Delphi 4 environment. Results of simulations of ferrite plate growth from supersaturated austenite isothermally treated in the temperature range of 250-400  $^{\circ}\text{C}$  are presented in **Fig. 4**.

Results of simulations show significant effect of austempering temperature on the bainitic ferrite growth. With increasing austempering temperature increases the rate,  $v$ , of plate thickness of ferrite. The relationship between  $v$  and time. It is necessary to emphasize, that during calculations of transformation progress the boundary condition (5) had to be modified assuming that carbon content in the middle of ferrite plate was equal  $0,95C_{\alpha/\gamma}$ . With (5) boundary condition ferrite plate thickness,  $l_{\alpha}$  was one order lower. Comparison of calculations using carbon content  $C$  and temperature  $T$  (on diffusion coefficient of carbon in austenite  $D(C, T)$ ) showed low effect on  $l_{\alpha}$ , increasing with austempering temperature (**Fig. 4a**).

Presented model will be developed with taking into account the rate nucleation of ferrite and full progress of austenite ferrite transformation during austempering. The calculated data will be experimentally verified.

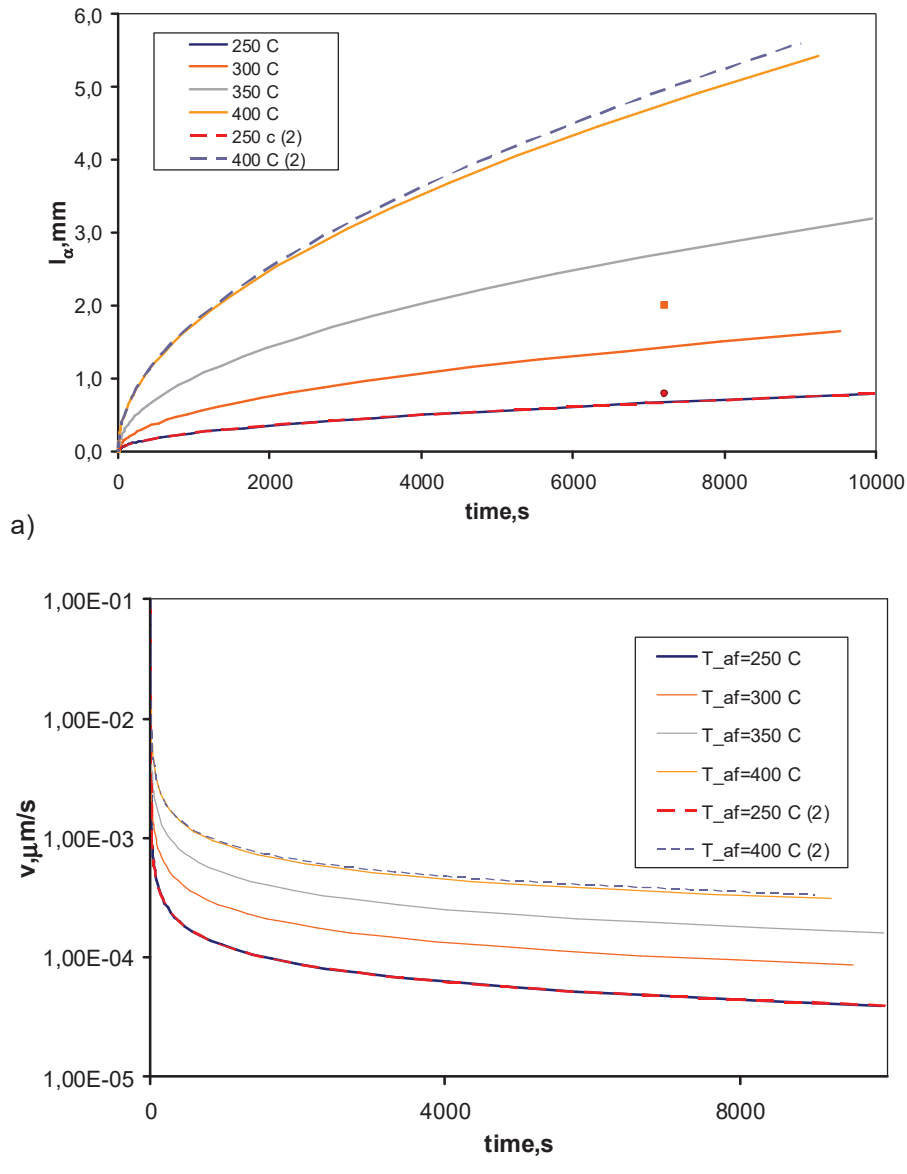


**Fig. 4** Results of ferrite growth simulation from austenite annealed at 850 °C and transformed in temperature range of 250-400 °C a) the relationships between a) ferrite plate thickness, b) rate of growth and austempering time. Dotted lines were calculated using  $D(C, T)$  relationship [8, 19]. Points - experimental data [17]

**ACKNOWLEDGEMENTS**

*Financial assistance of the NCN, project No. 2013/11/N/ST8/00326*

**REFERENCES**

[1] PODRZUCKI C. Żeliwo. Struktura, własności, zastosowanie, t.I i II, Wyd ZG STOP, Kraków, 1991.

- [2] ELLIOTT R., Current status of austempered cast irons, *Physical Metallurgy of Cast Iron V*, France, 1994, pp. 1-15.
- [3] AKBAY T., REED R., ATKINSON C. *Acta Metall. Mater.*, Vol. 42, 1994, pp. 1469-1480.
- [4] ZANARDI F. *Machinable ADI In Italy*. AFS Transactions, 2005, pp. 383-392.
- [5] PACYNA J. *Metaloznawstwo wybrane zagadnienia*, WND AGH, Kraków 2005.
- [6] ADRIAN H., *Numeryczne modelowanie procesów obróbki cieplnej*, Wydawnictwa AGH, Kraków 2011.
- [7] OLEJARCZYK-WOZENSKA I., ADRIAN H., WILK-KOŁODZIEJCZYK D., KLUSKA - NAWARECKA S. Numerical model of pearlite - austenite transformation. In *Metal 2014: 23rd International Conference on Metallurgy and Materials*. Ostrava, TANGER, 2014, pp. 611 - 617.
- [8] OLEJARCZYK-WOZENSKA, I. ADRIAN, H. MRZYGLÓD, B. Mathematical model of the process of pearlite austenitization, *Archives of Metallurgy and Materials*, Vol. 59, No. 3, 2014, pp. 981-986.
- [9] GŁOWACKI M. DEBINSKI T. OLEJARCZYK-WOZENSKA I. Fast parallel computation algorithm in application to simulation of semi-solid steel rolling and inverse analysis of its properties. *Numerical Analysis and Applied Mathematics*, Vol. 1558, 2013, pp. 2179-2182.
- [10] OLEJARCZYK-WOŻEŃSKA I., ADRIAN A., ADRIAN H., MRZYGLÓD B. Parametric representation of TTT diagrams of ADI cast iron. *Archives of Metallurgy and Materials*, Vol. 57, No. 2, 2012, pp. 613-617.
- [11] OLEJARCZYK-WOŻEŃSKA I., ADRIAN A., ADRIAN H., MRZYGLÓD B. Algorithm for controlling of quench hardening process of constructional steels. *Archives of Metallurgy and Materials*, Vol. 55, No. 1, 2010, pp. 171-179.
- [12] REGULSKI K., ROJEK G., SKÓRA M., KUSIAK J. Data exploration approach in control of metal forming manufacturing chain : example of fasteners production. In *Metal Forming 2012 :the 14th international conference on Metal Forming*, Steel Research International - spec. ed., 2012, pp. 1319-1322.
- [13] KLUSKA-NAWARECKA S., WILK-KOŁODZIEJCZYK D., REGULSKI K., DOBROWOLSKI G. Rough sets applied to the Rough Cast system for steel castings, *Intelligent Information and Database Systems. Part II*. In the third International Conference, ACIIDS 2011, Series: Springer Lecture Notes in Computer Science, Vol. 6592/2011, Daegu, Korea, 2011.
- [14] WOŹNIAK D., GŁOWACKI M., HOJNY M., PIEJA T. Application of CAE systems in forming of draw pieces with use rubber-pad forming processes. *Archives of Metallurgy and Materials*, Vol. 57, No. 4, 2012, pp. 1179-1187.
- [15] DĘBIŃSKI T., GŁOWACKI M., HOJNY M., GUMUŁA A., WOŹNIAK D. Web system dedicated to parallel computation for modelling of mushy steel deformation. *Archives of Metallurgy and Materials*, Vol. 59, No. 3, 2014, pp. 865-870.
- [16] WOŹNIAK D., GŁOWACKI M., ŻABA K., JĘDRZEJCZYK D., NOWOSIELSKI M. Application of numerical and photogrammetric systems to verification of tools designated for deep drawing process. In *Metal 2014: 23rd International Conference on Metallurgy and Materials*. Ostrava, TANGER, 2014, pp. 1534-1539.
- [17] KAPTURKIEWICZ W., BURBELKO A. A., LELITO J., FRAS E. Modelling of ausferrite growth in ADI. *International Journal of Cast Metals Research*, Vol. 16, 2003, pp. 287 - 292.
- [18] MURRAY D., LANDIS F. *Trans. Am. Soc. Min. Engrs.*, Vol. 81, 1959, pp. 106- 112.
- [19] BHADESHIA H. Diffusion of carbon in austenite. *Metal Sci.*, Vol. 15, 1981, pp. 477 - 479.